

Intracranial microvascular imaging at 7T MRI : A comparison of the different RF coils

Myung-Kyun Woo¹, Chang-Ki Kang¹, Suk-Min Hong¹, Kyoung-Nam Kim¹, Joshua Park¹, Hongbae Jeong¹, Hongbae Jeong¹, Hongbae Jeong¹, Young-Bo Kim¹, and Zang-Hee Cho¹

¹Neuroscience Research Institute, Gachon University, Incheon, Korea, Republic of

INTRODUCTION: MRA applications have been mainly limited to the volume coil, as it has relatively high sensitivity on the center of the brain compared with the periphery, although some studies have utilized multichannel coils [1]. However, dedicated RF coil designs for vascular imaging in ultra-high-field MRI are rare, particularly in the area of high-resolution MRA, which requires the optimization of SNR, uniformity, and penetration depth [2,3]. The purpose of the present study was the identification of the most suitable RF coil for neuromicrovascular imaging, where deepest penetration depth to the center of the brain, high SNR, and possibility of parallel imaging are critically important.

MATERIALS and METHODS: All imaging tests were performed on a prototype 7T human scanner (Siemens). We used RediFoam (Med-Tec) to insure subject immobilization and experimental replication. Five coils were developed: a volume coil - a hybrid birdcage coil that acted as a template (Fig. 1(a)), a 4-channel (4-CH) coil (Fig. 1(b)), an overlapped 4-ch coil (4-CH OV) (Fig. 1(c)), an overlapped 6-ch coil (6-CH OV) (Fig. 1(d)), and an overlapped 8-ch coil (8-CH OV) (Fig. 1(e)). For the present study, each coil with a diameter of 24 cm was constructed to accommodate the human head. The length of the rung of the hybrid birdcage coil was 13 cm and the RF coil consisted of 16 rungs (a). The coil loop dimensions were $17 \times 13 \text{ cm}^2$ (b), $22.5 \times 15 \text{ cm}^2$ (c), $15 \times 15 \text{ cm}^2$ (d) and $12.5 \times 15 \text{ cm}^2$ (e). Quality factor (Q_U for unloaded and Q_L for loaded) for each coil configuration was recorded a single element in isolation and with the ratio of unloaded to loaded Q (Q_U / Q_L) was calculated for the individual coil. Q_U , Q_L and the ratio were 3.6 (4-CH), 3.5 (4-CH OV), 4.0 (6-CH OV), and 3.8 (8-CH OV), respectively.

Experiments and Analysis: We investigated the properties of penetration depth of each coil conducting phantom imaging and in-vivo study, acquiring a T1 magnetization-prepared rapid acquisition using gradient echo (MPRAGE) images. Then, the penetration depth of the coils was examined with the SNR profiles of MPRAGE images obtained by each coil. The SNR was calculated with the signal divided by a standard deviation of background noise. For microvascular imaging, we employed MR parameters similar to those reported previously. For microvascular imaging, a three-dimensional fast low-angle shot (FLASH) gradient-echo sequence was used with a single slab. A targeted maximum intensity projection (MIP) image was made and designated as a region of interest (ROI), which was focused on the main trunk of the middle cerebral artery and the anterior cerebral artery. The resulting angiogram for microvessels was displayed on the coronal view. The sequence parameters were 2500ms/2.8ms/128x128/1.8mm (TR/TE/matrix/slice thickness) for MPRAGE and 15/4.78/580x640/0.36 and 17/5.05/714x768/0.3 for lower- and higher-resolution FLASH, respectively.

RESULTS and DISCUSSION: The penetration depth was also measured quantitatively using the SNR profiles of each coil (Fig. 2). The 4-CH OV and 6-CH OV coils had larger penetration depth and higher SNR than 4-CH coil. Overall, the 6-CH OV coil appeared to have the highest sensitivity at the center of the brain because it had the largest penetration depth (Fig. 2). From these plots, one could easily see that the 6-CH OV coil appeared to have the best performance, whereas the coil with a higher number of loop coils did not show increased SNR at the center of the brain, probably because of the reduced penetration depth. In addition to SNR and sensitivity, another important evaluation criterion for selecting the appropriate RF coil appears to be the resolving power in cerebral vascular imaging. To assess this parameter, we compared the resolving power of microvascular imaging at the central aspect of the brain on coronal MIP images, focusing specifically on the lenticulostriate arteries (LSAs) (Fig. 3). The birdcage coil could the highest vessel contrast at the center of the brain relative to the other coils (Fig. 3(a)). However, the LSAs' image from the 6-CH OV coil was comparable to that of the birdcage coil. This means that the 6-CH OV coil has high penetration depth or sensitivity and uniform vascular contrast throughout the brain. In contrast, the operation of coils at a lower resolution mode revealed that the 8-CH OV coil had lower resolving power, especially for LSAs (black arrows in Fig. 3). At a higher resolution mode the 6-CH OV coil provided superior overall performance in LSAs imaging with a given acquisition time compared with the other coils (white arrows in Fig. 3). The most important advantage of the 6-CH OV coil was found in higher resolution imaging, where substantial advantages are seen over the lower resolution mode (red arrows in Fig. 3). The overall sensitivity of the 6-CH OV coil was also much higher than other coils (see higher resolution profiles in Fig. 3). Note that GRAPPA was not applicable for LSAs with the birdcage coil. In conclusion, we have shown that the design of the most suitable RF coil is an important factor in high-resolution microvascular imaging or angiography for ultra-high-field MRI such as 7T MRI and the 6-CH OV coil appears to be the best suited choice for both penetration depth and SNR.

REFERENCES: [1] Wiggins GC et al. MRM 2005;54(1):235-240. [2] Wald LL et al. *Appl Magn Reson* 2005;29(1). [3]. Maderwald S et al. *Magma* 2008;21(1-2):159-167.

ACKNOWLEDGEMENT: This work is supported by the Original Technology Research Program for Brain Science through the National Research Foundation of Korea (NRF) (2008-2004159), Republic of Korea.

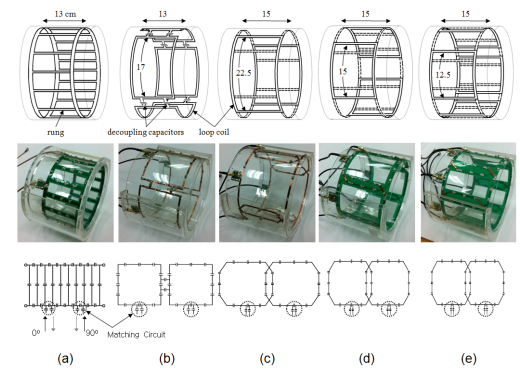


Fig.1. RF coil drawings and the corresponding photographs and coil circuit diagrams.

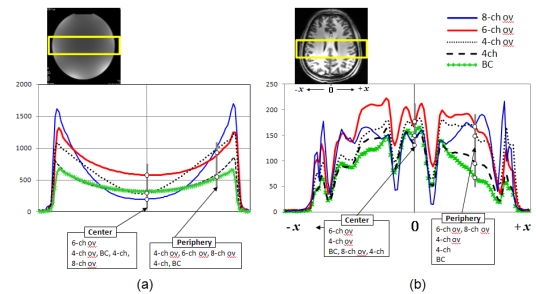


Fig 2. SNR profiles of RF coils measured from phantom (a) and human (b) T1 MPRAGE images.

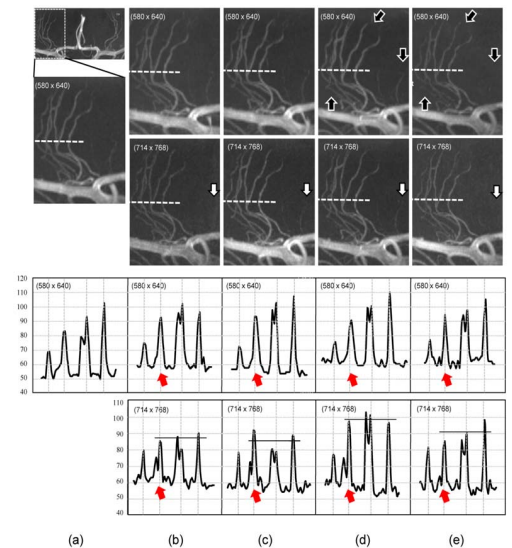


Fig 3. Coronal MIP images of each coil on the brain center and vascular profiles of microvessels (LSAs) (a) hybrid birdcage coil, (b) 4-CH coil, (c) 4-CH OV coil, (d) 6-CH OV coil and (e) 8-CH OV coil. Upper MRA images and profiles: lower resolution FLASH, Lower: higher resolution FLASH